Journal of Integrative Neuroscience

J. Integr. Neurosci. **2026**; 25(3): 46585
https://doi.org/10.31083/JIN46585

Original Research

Integrating Substantia Nigra Hyperechogenicity and Inflammation-Associated Biomarkers: A Classification Model for Staging Cognitive Impairment in Parkinson's Disease

Jiahang Zhao[1], Chao Hou[1,2], Sen Wang[1], Yiqun Lin[1], Linyu Xu[1], Wen He[1,*], Wei Zhang[1,*]

[1]Department of Ultrasound, Beijing Tiantan Hospital, Capital Medical University, 100070 Beijing, China
[2]Department of Ultrasound, The Affiliated Hospital of Southwest Medical University, 646000 Luzhou, Sichuan, China
*Correspondence: hewen@bjtth.org (Wen He); ultrazhangwei@126.com (Wei Zhang)
Academic Editors: Foteini Christidi and Bettina Platt
Submitted: 14 September 2025 Revised: 21 December 2025 Accepted: 5 January 2026 Published: 9 March 2026

Abstract

Background: Cognitive impairment (CI) is recognized as a debilitating complication of Parkinson's disease (PD). This study was designed to develop a diagnostic classification model by integrating substantia nigra hyperechogenicity (SNH) and inflammationassociated biomarkers to evaluate its diagnostic performance in distinguishing PD CI stages. **Methods**: Between January, 2023 and May, 2024, 184 patients with PD who underwent transcranial sonography were prospectively enrolled. Based on Montreal Cognitive Assessment (MoCA) scores, participants were categorized into three groups: cognitive impairment (PD-CI, MoCA <26), mild cognitive impairment (PD-MCI, MoCA 22–25), and dementia (PD-dementia, MoCA ≤21). Ultrasound features and inflammationassociated biomarkers were screened with univariate analyses. Multivariate logistic regression was used to identify independent diagnostic factors, and receiver operating characteristic (ROC) curve analysis was used to assess model discrimination. **Results**: Multivariate regression analysis indicated that age <50 years and more years of education were significantly associated factors for CI (OR = 0.170, $p = 0.0350$; OR = 0.8780, $p = 0.0020$, respectively), whereas Unified Parkinson's Disease Rating Scale Part III (UPDRSIII) score (OR = 1.024, $p = 0.0270$), SNH (OR = 2.550, $p = 0.0030$), elevated C-reactive protein (CRP) (OR = 2.038, $p = 0.0350$), and elevated homocysteine (Hcy) (OR = 2.830, $p = 0.0020$) were independent risk factors. The area uinder the curves (AUCs) for the combined SNH+CRP+Hcy model in predicting PD-CI, PD-MCI, and PD-dementia were 0.783, 0.729, and 0.823, respectively; these values were significantly superior to those for single or dual marker combinations ($p < 0.05$), with the strongest performance for distinguishing PD-dementia. **Conclusion**: An SNH and inflammationassociated biomarkerbased model was developed for predicting the stage of cognitive impairment in PD. Clinical targets for individualized intervention can be provided, and clinical risk stratification and care pathways can be optimized. Furthermore, the model supports the iron deposition-neuroinflammation-CI pathway hypothesis, providing a mechanistic rationale for ultrasoundbased PD-CI diagnosis.

Keywords: Parkinson's disease; cognitive impairment; substantia nigra; ultrasonography; inflammation

1. Introduction

Parkinson's disease (PD) is recognized as the most prevalent movement disorder worldwide and as the second most common neurodegenerative disease after Alzheimer's disease (AD) [1,2]. Beyond the cardinal motor symptoms (bradykinesia, rigidity, resting tremor), PD is characterized by heterogeneous non-motor sequelae, and cognitive impairment (CI) shows a sixfold higher prevalence than in age-matched controls [2]. CI substantially diminishes functional independence and quality-of-life measures in patients with PD, imposing socioeconomic burdens that exceed those of motor disability even during prodromal phases [3,4]. Accordingly, early diagnostic and identification of CI are essential for PD management.

Neuroinflammation is recognized as a core pathological mechanism in PD. It affects not only the substantia nigra (SN) and striatum but also cognition-related regions such as the frontal lobe and hippocampus, thereby contributing to CI [5–7]. This process is amplified by peripheral metabolic disturbances, in which homocysteine (Hcy) accumulation—mediated by deficiencies of the cofactors folate (FA) and vitamin B12 (VB12)—induces excitotoxicity via N-methyl-D-aspartate (NMDA) receptor overactivation and impairs DNA repair in cognitive circuits [8–10]. Concurrently, iron dyshomeostasis, reflected by elevated ferritin (Fer), potentiates microglial activation and lipid peroxidation, thereby exacerbating neuronal vulnerability through ferroptotic pathways. The resulting oxidative milieu depletes endogenous antioxidants such as uric acid (UA), further diminishing neuroprotection and accelerating cognitive decline [11–13]. Systemic inflammation is evidenced by elevated C-reactive protein (CRP), which correlates with blood-brain barrier disruption and microglial priming [14], whereas neuron-specific enolase

Copyright: © 2026 The Author(s). Published by IMR Press.
This is an open access article under the CC BY 4.0 license.

Publisher's Note: IMR Press stays neutral with regard to jurisdictional claims in published maps and institutional affiliations.

(NSE) serves as a surrogate marker of neuronal damage in cortico-limbic networks [15,16]. These peripheral biomarkers appear mechanistically interlinked: elevations in Hcy (due to FA/VB12 deficiency) synergize with iron overload (high Fer) to amplify mitochondrial reactive oxygen species (ROS) generation, which in turn depletes UA and upregulates CRP, creating a pathological feed-forward loop that drives neuroinflammation and CI. Therefore, neuroinflammation-related peripheral biomarkers may help in the diagnosis of CI in PD.

Transcranial sonography (TCS) has emerged as a noninvasive neuroimaging tool, and substantia nigra hyperechogenicity (SNH) has been validated as an imaging biomarker of nigrostriatal pathology in PD [17]. SNH can be detected in prodromal PD and persists throughout disease progression. Although current TCS research predominantly examines associations between SNH and measures of PD duration or severity, its utility for predicting cognitive impairment has been underexplored [18,19].

Given the neuroinflammatory heterogeneity underlying CI in PD and the diagnostic advantages of TCS-identified high echogenicity in the SN, SNH, and multisource inflammation markers were integrated to identify individuals at increased risk of early, rapid cognitive decline. This approach is intended to enhance diagnostic stratification and to support the implementation of precision-prevention protocols.

2. Methods

2.1 Patients

Data on patients with PD treated in the Movement Disorders Department who underwent TCS between January 2023 and May 2024 were prospectively collected. The diagnosis of PD was made according to the International Parkinson's and Movement Disorder Society criteria [20]. Antiparkinsonian medications were withheld for at least 12 hours before clinical assessment. Exclusion criteria included atypical Parkinsonian syndromes, secondary Parkinsonism, other non-Parkinsonian disorders, incomplete clinical records, an inadequate temporal bone window for TCS, indeterminate ultrasound findings, or a history of brain surgery or traumatic brain injury.

2.2 Cognitive and Behavioral Assessments

Neurological evaluations were performed by two board-certified neurologists, each with more than five years of experience in movement disorders, using the Movement Disorder Society-Unified Parkinson's Disease Rating Scale (MDS-UPDRS). In instances of discordant evaluations, the final diagnosis was adjudicated by a senior specialist with more than ten years of experience in movement disorders. Global cognitive function was assessed with the Montreal Cognitive Assessment (MoCA) [21], following guidelines from the International Parkinson and Movement Disorder Society; total scores range from 0 to 30, with values <26 indicating CI [21,22]. Cognitive status was classified into three groups: normal cognition (MoCA ≥ 26), mild cognitive impairment (MCI; MoCA 22–25), and dementia (MoCA ≤ 21) [23].

2.3 TCS Examination

Hyperechoic areas of the SN were identified and measured by two experienced sonographers, each with more than ten years of neuroimaging experience, who were blinded to the patients' clinical diagnoses. A Canon Aplio i900 system (Canon Medical Systems Corporation, Ōta, Tokyo, Japan) equipped with a 2.0–3.0 MHz phased-array transducer (I6SX1) was used. Standardized parameters included a scan depth of 14–16 cm and a dynamic range of 45–55 dB, with real-time adjustments to gain compensation and brightness tailored to individual anatomy.

With the patient in the supine position and the temporal acoustic window fully exposed, the phased-array transducer was placed over the temporal region. Systematic midbrain exploration was performed by incrementally angling the ultrasound beam along the orbitomeatal line (connecting the lateral canthus and external auditory meatus). Once the characteristic butterfly-shaped midbrain morphology adjacent to the midline was identified, peripheral and internal nuclei were assessed when bone-window penetration permitted adequate visualization. SNH was documented when present in the ipsilateral or contralateral SN. SN echogenicity was graded according to the standardized Bartova classification [24], and interrater reliability for SNH area quantification and grading was assessed using intraclass correlation coefficients (ICCs).

2.4 Clinical Data Collection

Comprehensive baseline clinical data were collected for all participants, including sex, age, disease duration, years of formal education, and disease severity assessed by the modified Hoehn and Yahr (H-Y) stage. Motor symptom severity was evaluated using the Movement Disorder Society-Unified Parkinson's Disease Rating Scale Part III (UPDRS-III), and global cognitive function was screened with the MoCA. Comorbidity status was documented for hypertension, hyperlipidemia, and diabetes mellitus. Anthropometric data included body mass index (BMI), along with self-reported smoking status and alcohol consumption patterns. Age was categorized into <50 years, 50–69 years, 70–74 years, and ≥ 75 years.

Serum biomarkers related to neuroinflammation and metabolic pathways were quantified from venous blood collected under standardized fasting conditions using validated immunoassay techniques. The panel included FA, VB12, Fer, CRP, NSE, UA, and Hcy. For analysis, each biomarker was dichotomized into normal or abnormal based on established clinical reference ranges. Normal ranges were defined as: FA ≥ 5 ng/mL; VB12 211–911 pg/mL; Fer 10–291 ng/mL; CRP ≤ 2.87 mg/L; NSE ≤ 19.68 ng/mL; UA 142–416 µmol/L; and Hcy ≤ 15 µmol/L.

2.5 Statistical Analysis

Statistical analyses were conducted using SPSS v21.0 (IBM Corp., Armonk, NY, USA). Continuous variables were expressed as mean ± SD (normally distributed) or median with interquartile range (IQR) (non-normally distributed), with normality assessed via the K-S test. Group comparisons employed an independent samples *t*-test (parametric) or a Mann-Whitney U test (non-parametric) for continuous variables, and a χ^2 test or Fisher's exact test for categorical variables. Multivariate ordinal logistic regression identified independent predictors of CI, with variables selected based on clinical relevance and univariate screening ($p < 0.10$). Model performance was evaluated using receiver operating characteristic (ROC) curve analysis (area under the curve [AUC] quantification).

Missing data management: Variables with >30% missingness were excluded; those with ≤10% missingness were imputed using median (non-normal continuous), mean (normal continuous), or mode (categorical variables). Sample size adequacy satisfied the 5–10 cases per predictor variable criterion for regression stability. Statistical significance was defined as two-tailed $p < 0.05$.

3. Results

3.1 Univariate Analysis

3.1.1 Patient Selection and Demographics

Between January 2023 and May 2024, 647 patients were enrolled in this study. Following screening, 463 patients were excluded: Parkinsonism (n = 230), non-Parkinsonism (n = 139), ambiguous SN findings on TCS examination (n = 90), history of Traumatic Brain Injury (n = 1), and history of deep brain stimulation (DBS) surgery (n = 3); a detailed flowchart of the patient selection process is presented in Fig. 1. Consequently, 184 patients met the inclusion criteria and were analyzed in this study. Among the 184 patients analyzed, 16 had ≤10% missingness, which were imputed according to the predefined protocol (**Supplementary Table 1**). The final cohort consisted of 120 males (65.2%) and 64 females (34.8%). The mean age was 63.06 ± 9.56 years. The mean score on the MoCA was 21.11 ± 5.34, 2.13 ± 0.87 for H-Y stage, 38.46 ± 15.34 for UPDRS-III, and 6.57 ± 4.59 years for disease duration (Fig. 1).

3.1.2 Baseline Characterization

Based on MoCA scores, the participants were stratified as follows: 42 subjects demonstrated normal cognitive function (MoCA score ≥26), 60 subjects were classified as having MCI (MoCA score 22–25), and 82 subjects were classified as having dementia (MoCA score ≤21). Univariate analysis revealed statistically significant differences in H-Y stage, years of formal education, and UPDRS-III scores. Conversely, no statistically significant differences were observed for sex, BMI, disease duration, hypertension, hyperlipidemia, diabetes mellitus, self-reported smoking status, or alcohol consumption patterns (all $p > 0.05$) (Table 1).

3.1.3 Serum and Imaging Indicators

TCS assessment of the SN revealed statistically significant findings ($p = 0.0020$). Among inflammatory-associated biomarkers, significant differences were observed for CRP and Hcy ($p = 0.0001$ and $p = 0.0030$, respectively). In contrast, no statistically significant differences were found for FA, VB12, Fer, NSE, or UA (all $p > 0.05$) (Table 2, Fig. 2).

3.2 Multifactorial Logistic Regression Analysis

Variables exhibiting a significant association ($p < 0.10$) in the univariate analysis were included in the multivariable logistic regression model. The covariates entering the multivariate model were: Age, years of formal education, H-Y stage, UPDRS-III, SNH, CRP, Hcy, and FA (Table 2). Multivariable logistic regression analysis of age, education level, UPDRS-III score, SNH, Hcy, and CRP as independent predictors of CI. Univariate *p*-values are reported unadjusted and serve as exploratory screening criteria only. Final statistical inference is based on the multivariable ordinal logistic regression model (all $p < 0.05$, two-sided).

3.3.1 Baseline Characterization

Participants younger than 50 years exhibited an 83.0% reduced risk of CI compared to those aged ≥75 years (OR = 0.170, $p = 0.0350$). Similarly, longer formal education duration was a significantly associated factor against CI. For each additional year of education, the adjusted odds of CI decreased by 12.2% (OR = 0.878, $p = 0.0020$). Although the UPDRS-III effect size appears modest (OR = 1.024), its cumulative impact may be clinically significant in individuals with high scores. The precisely estimated 95% confidence interval (CI: 1.003–1.046) confirms a statistically significant positive association with cognitive impairment risk, corresponding to a 2.4% increase in risk per 1-point increase in score (Table 3).

3.3.2 Serum and Imaging Biomarkers

Elevated CRP independently predicted CI (OR = 2.038, $p = 0.0350$), conferring a 2.04 times increased risk. Hcy elevation was associated with a highly significant risk (OR = 2.830, $p = 0.0020$), indicating a 2.83 times higher CI risk. Further, SNH was an independent risk factor for CI, with positive cases having a 2.55-fold higher risk than negative cases (OR = 2.550, $p = 0.0030$) (Table 3).

3.3.2.1 PD-NC (MoCA score ≥26) vs. PD-CI (MoCA score <26). To evaluate the ability of the three independent predictors to identify PD-CI, we performed ROC curve analysis. The AUC for the single predictors SNH, CRP, and

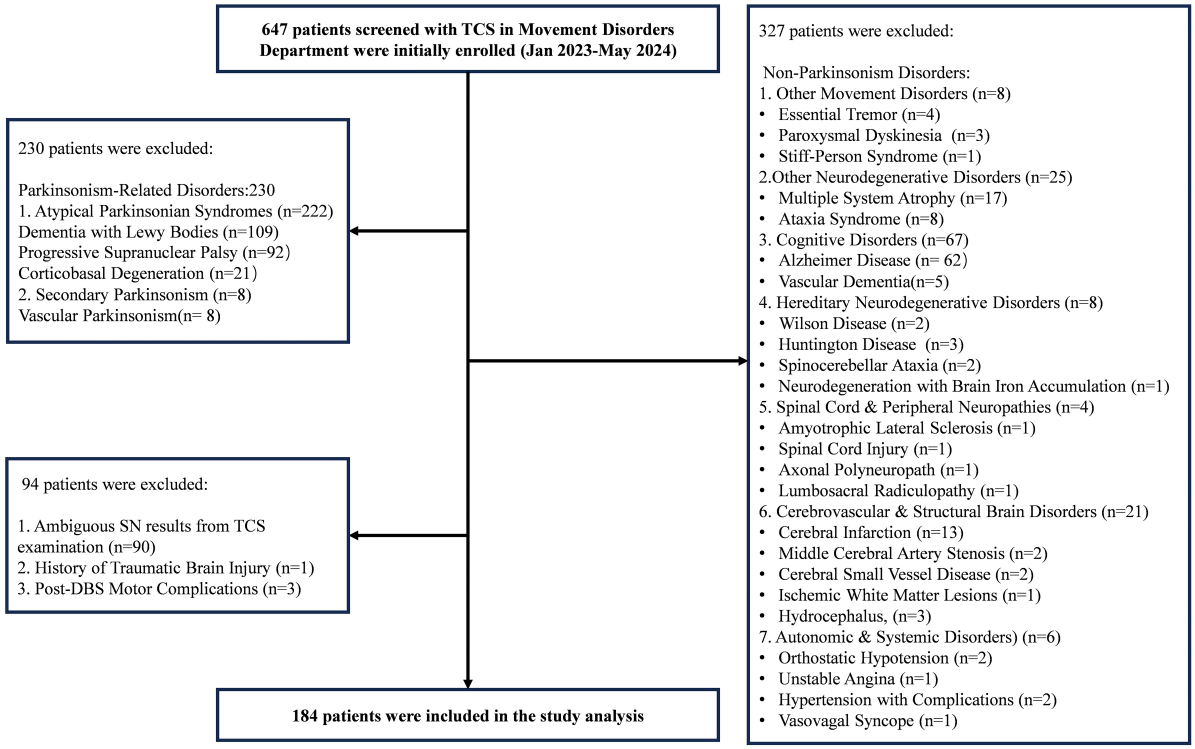

Fig. 1. Study flow chart. DBS, deep brain stimulation; SN, substantia nigra; TCS, transcranial sonography.

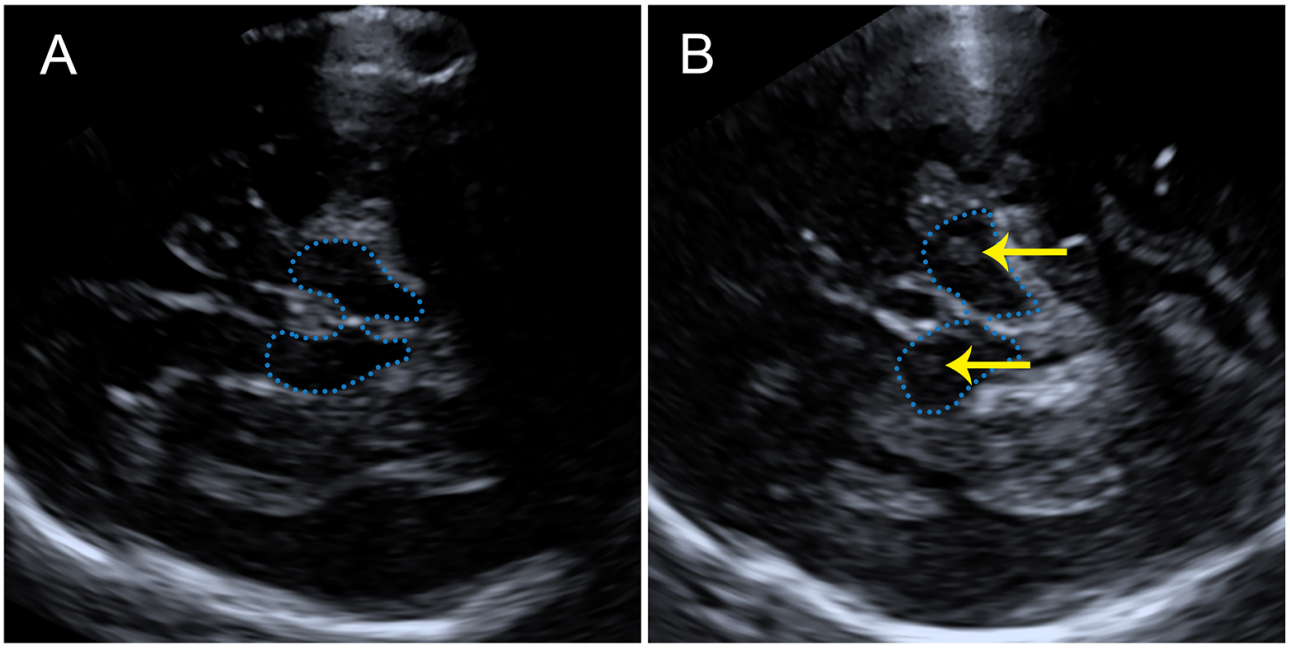

Fig. 2. Transcranial ultrasonography showing butterfly-shaped midbrain and internal sonographic features. (A) No significant substantia nigra hyperechogenicity (SNH) is detected within the midbrain. (B) Focal SNH is visualized within the midbrain (yellow arrow). The blue dashed line outlines the midbrain region.

Hcy was 0.636, 0.655, and 0.646, respectively. Pairwise comparison analysis revealed no statistically significant differences in AUC values among these individual biomarkers (all $p > 0.05$). Although their diagnostic performance was comparable, the performance characteristics differed: SNH demonstrated moderate sensitivity (60.56%) and specificity (66.67%), whereas CRP and Hcy exhibited higher specificity (88.10% and 83.33%, respectively) (Table 4, Fig. 3).

Table 1. Baseline characterization of participants.

Variables	PD-NC (n = 42)	PD-MCI (n = 60)	PD-dementia (n = 82)	$\chi^2/t/z$	p
Age				11.916	0.064
<50	6	5	2		
50–69	24	47	56		
70–74	9	5	16		
≥75	3	3	8		
Sex (male)				0.390	0.823
Male	27	41	52		
Female	15	19	30		
BMI (kg/m^2)	24.88 ± 3.59	24.15 ± 3.44	24.54 ± 3.50	6.815	0.575
Duration of disease (years)	5.82 ± 3.92	6.94 ± 4.13	6.68 ± 5.19	2.084	0.353
Education level (years)	11.95 ± 3.61	11.60 ± 3.17	9.17 ± 4.36	16.684	<0.001
UPDRS-III	32.31 ±13.29	38.10 ± 15.06	41.87 ± 15.68	5.687	0.004
H-Y stage	1.95 ± 0.84	1.98 ± 0.77	2.32 ± 0.92	9.230	0.010
Smoking				0.277	0.871
Yes	9	15	21		
No	33	45	61		
Drinking alcohol				2.599	0.273
Yes	9	21	21		
No	33	39	61		
Hypertension				4.585	0.101
Yes	17	15	34		
No	25	45	48		
Dyslipidemia				0.167	0.920
Yes	6	10	14		
No	36	50	68		
Diabetes mellitus				0.292	0.864
Yes	14	17	25		
No	28	43	57		

H-Y stage, Hoehn and Yahr stage; PD, Parkinson's disease; PD-dementia, PD patients with dementia; PD-MCI, PD patients with mild cognitive impairment; PD-NC, PD patients with normal cognitive function; UPDRS-III, Unified Parkinson's Disease Rating Scale Part III; BMI, body mass index.

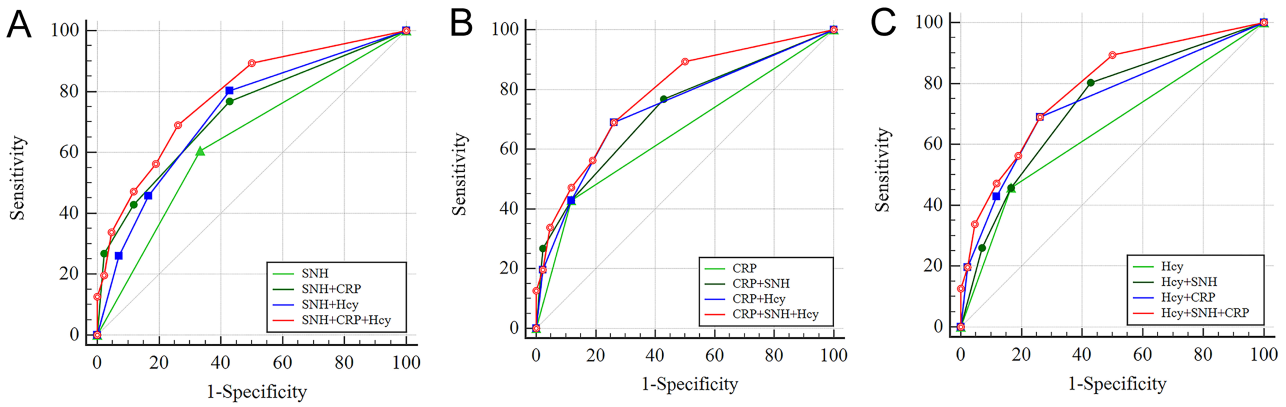

Fig. 3. Receiver operating characteristic curve of models predicting the CI of PD. (A) SNH-related diagnostic classification model. (B) CRP-related diagnostic classification model. (C) Hcy-related diagnostic classification model.

Given the limitations of single predictors, we explored the diagnostic performance of different indicator combinations. SNH+CRP model and SNH+Hcy model resulted in increased sensitivity 76.76%, 80.28%, respectively) compared to any single-indicator model, with AUCs also improving to an upper-moderate level (0.727, 0.724, respectively). Conversely, the CRP+Hcy model exhibited a different trend, achieving an AUC of 0.736, a sen-

Table 2. Serum and imaging indicators of participants.

Variables	PD-NC (n = 42)	PD-MCI (n = 60)	PD-dementia (n = 82)	$\chi^2/t/z$	p
SNH				13.001	0.002
Present	14	31	55		
Absent	28	29	27		
FA				4.935	0.085
Decreased	9	24	33		
Normal	33	36	49		
VB12				3.763	0.439
Increased	4	5	7		
Decreased	2	9	6		
Normal	36	46	69		
Fer				2.097	0.351
Increased	0	2	4		
Normal	42	58	78		
CRP				15.375	<0.001
Increased	5	22	39		
Normal	37	38	43		
NSE				4.239	0.120
Increased	4	9	4		
Normal	38	51	78		
UA				1.688	0.430
Increased	4	2	5		
Normal	38	58	77		
Hcy				11.790	0.003
Increased	7	26	39		
Normal	35	34	43		

CRP, C-reactive protein; FA, folic acid; Fer, ferritin; Hcy, homocysteine; NSE, neuron-specific enolase; UA, uric acid; VB12, vitamin B12.

Table 3. Multivariate analysis for predicting stages of cognitive impairment (CI) for PD.

Variables	B	SE	Wald test	OR (95% CI)	p
Age (years)					
<50	–1.775	0.840	4.469	0.170 (0.033–0.879)	0.035
50–69	–0.442	0.604	0.537	0.642 (0.197–2.099)	0.464
70–74	–0.864	0.687	1.581	0.422 (0.110–1.621)	0.209
≥75	-	-	-	-	-
Education level (years)	–0.130	0.043	9.299	0.878 (0.808–0.955)	0.002
H-Y stage	–0.027	0.200	0.018	0.973 (0.658–1.441)	0.893
UPDRS-III	0.024	0.011	4.921	1.024 (1.003–1.046)	0.027
SNH	0.936	0.314	8.885	2.550 (1.378–4.721)	0.003
CRP	0.712	0.337	4.460	2.038 (1.052–3.945)	0.035
Hcy	1.040	0.335	9.660	2.830 (1.469–5.453)	0.002
FA	0.268	0.341	0.620	1.308 (0.671– 2.550)	0.431

B, regression coefficient; SE, standard error.

sitivity of 69.01%, and a specificity increased to 73.81%. The comprehensive model combining all three indicators (SNH+CRP+Hcy) showed the highest AUC among the models evaluated for PD-CI. This model's AUC improved significantly to 0.783, surpassing the performance of all single- and dual-indicator models. Compared to the dual-marker models, its specificity was significantly enhanced, reaching 73.81%. The lower limit of the model's 95% confidence interval (CI: 0.707–0.859) was above the chance level (0.5), and the narrow 95%CI suggests stable estimates, indicating good discriminatory ability for distinguishing PD-CI from PD patients with normal cognitive function (PD-NC) (Table 4, Fig. 3).

3.3.2.2 PD-NC (MoCA score ≥26) vs. PD-MCI (MoCA score 22–25). The diagnostic performance of the indica-

Table 4. Diagnostic performance of models to predict PD-CI.

Variables	Sensitivity	Specificity	AUC (95% CI)	$^{\dagger}p$	$^{\ddagger}p$	$^{\S}p$
SNH	60.56	66.67	0.636 (0.553–0.719)	-	-	-
CRP	42.96	88.10	0.655 (0.591–0.719)	0.728	-	-
Hcy	45.77	83.33	0.646 (0.575–0.716)	0.862	0.840	-
SNH+CRP	76.76	57.14	0.727 (0.651–0.803)	0.018	0.004	-
SNH+Hcy	80.28	57.14	0.724 (0.640–0.807)	0.028	-	0.001
CRP+Hcy	69.01	73.81	0.736 (0.662–0.810)	-	<0.001	0.010
SNH+CRP+Hcy	69.01	73.81	0.783 (0.707–0.859)	0.001	<0.001	<0.001

$^{\dagger}p$, p-value obtained by comparing SNH with row headers; $^{\ddagger}p$, p-value obtained by comparing CRP with row headers; $^{\S}p$, p-value obtained by comparing Hcy with row headers.

Table 5. Diagnostic performance of models to predict PD-MCI.

Variables	Sensitivity	Specificity	AUC (95% CI)	$^{\dagger}p$	$^{\ddagger}p$	$^{\S}p$
SNH	51.67	66.67	0.592 (0.495–0.688)	-	-	-
CRP	36.67	88.10	0.624 (0.545–0.703)	0.611	-	-
Hcy	43.33	83.33	0.633 (0.548–0.718)	0.526	0.867	-
SNH+CRP	36.67	57.14	0.666 (0.569–0.764)	0.089	0.185	-
SNH+Hcy	75.00	57.14	0.692 (0.593–0.791)	0.037	-	0.047
CRP+Hcy	61.67	73.81	0.695 (0.604–0.787)	-	0.014	0.123
SNH+CRP+Hcy	61.67	73.81	0.729 (0.633–0.824)	0.011	0.005	0.019

$^{\dagger}p$, p-value obtained by comparing SNH with row headers; $^{\ddagger}p$, p-value obtained by comparing CRP with row headers; $^{\S}p$, p-value obtained by comparing Hcy with row headers.

tors was evaluated using ROC curve analysis. The AUC values for the individual indicators SNH, CRP, and Hcy were 0.592, 0.624, and 0.633, respectively. Pairwise comparisons indicated no statistically significant differences in the AUCs of these indicators (all $p > 0.05$). While demonstrating moderate overall diagnostic performance, each indicator exhibited relatively high specificity: 66.67% for SNH, 83.33% for Hcy, and 88.10% for CRP (Table 5, Fig. 4).

Combination models significantly enhanced diagnostic performance compared to single-indicator models. Among dual-indicator models, the SNH+Hcy model yielded the highest sensitivity (75.00%), albeit with lower specificity (57.14%). In contrast, the CRP+Hcy model maintained relatively high specificity (73.81%) while providing a more balanced sensitivity (61.67%), achieving the higher AUC among dual-indicator models (0.695). Notably, the integrated SNH+CRP+Hcy model demonstrated superior overall diagnostic performance (AUC = 0.729), exceeding those of single-indicator and several dual-indicator models. It achieved balanced performance with a sensitivity of 61.67% and a specificity of 73.81%. The lower limit of its 95% confidence interval (0.633) was notably above the chance level (0.5), further validating the better diagnostic performance of this SNH+CRP+Hcy model for differentiating between PD-NC and PD-MCI (Table 5, Fig. 4).

3.3.2.3 PD-NC (MoCA $\geq$26) vs. PD-dementia (MoCA $\leq$21). ROC curve analysis revealed AUC values for the single indicators SNH, CRP, and Hcy of 0.669, 0.678, and 0.654, respectively, with no statistically significant differences between them. Among the single-indicator tests, SNH demonstrated the highest sensitivity (67.07%), while CRP and Hcy exhibited superior specificity (88.10% and 83.33%, respectively) (Table 6, Fig. 5).

Notably, the SNH+CRP model and the SNH+Hcy model achieved substantially higher sensitivity (84.15% for both), though with reduced specificity (57.14% for both). The AUCs for these dual-indicator models were significantly higher than those of the single-indicator model (SNH+CRP: AUC = 0.771; SNH+Hcy: AUC = 0.747). The CRP+Hcy model maintained relatively high specificity (73.81%) while providing reasonable sensitivity (74.39%), yielding an AUC of 0.766 (Table 6, Fig. 5).

Most importantly, the SNH+CRP+Hcy model demonstrated the best diagnostic efficacy. Its AUC increased significantly to 0.823 while maintaining sensitivity of 74.39% and specificity of 73.81%, demonstrating a balance of performance characteristics and solid discriminatory power. The lower limit of this model's 95% confidence interval (CI: 0.747–0.899) substantially exceeded the chance level (0.5), further confirming its reliable diagnostic performance for distinguishing PD-NC from PD-dementia (Table 6, Fig. 5).

4. Discussion

This study developed a diagnostic classification model by combining SNH with serum inflammation-associated

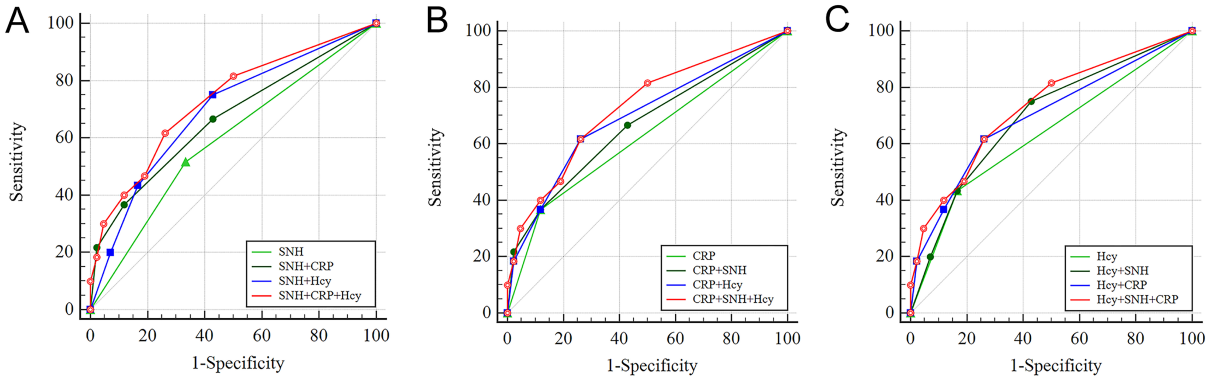

Fig. 4. Receiver operating characteristic curve of models predicting the MCI of PD. (A) SNH-related diagnostic classification model. (B) CRP-related diagnostic classification model. (C) Hcy-related diagnostic classification model.

Table 6. Diagnostic performance of models to predict PD- dementia.

Variables	Sensitivity	Specificity	AUC (95% CI)	$^{\dagger}p$	$^{\ddagger}p$	$^{\S}p$
SNH	67.07	66.67	0.669 (0.580–0.757)	-	-	-
CRP	47.56	88.10	0.678 (0.605–0.752)	0.875	-	-
Hcy	47.56	83.33	0.654 (0.576–0.733)	0.811	0.669	-
SNH+CRP	84.15	57.14	0.771 (0.691–0.851)	0.019	<0.001	-
SNH+Hcy	84.15	57.14	0.747 (0.659–0.835)	0.069	-	<0.001
CRP+Hcy	74.39	73.81	0.766 (0.685–0.846)	-	<0.001	0.006
SNH+CRP+Hcy	74.39	73.81	0.823 (0.747–0.899)	0.002	<0.001	<0.001

$^{\dagger}p$, p-value obtained by comparing SNH with row headers; $^{\ddagger}p$, p-value obtained by comparing CRP with row headers; $^{\S}p$, p-value obtained by comparing Hcy with row headers.

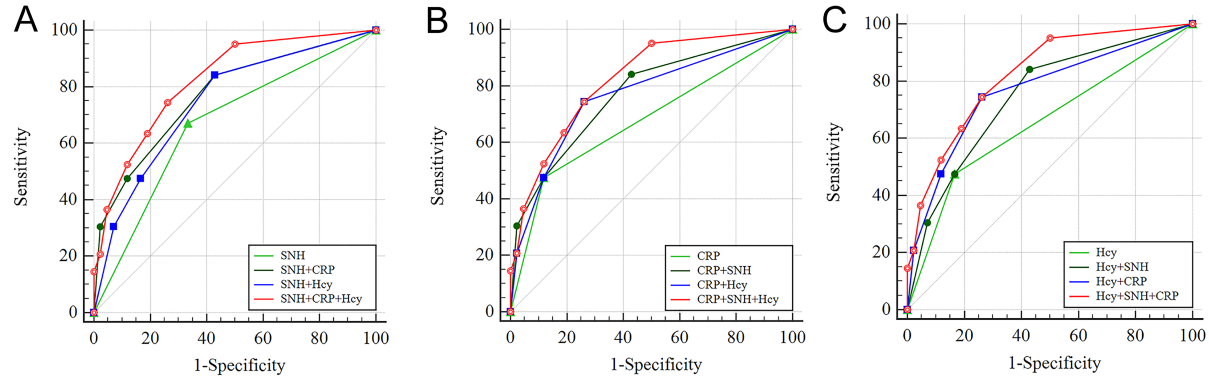

Fig. 5. Receiver operating characteristic curve of models predicting the dementia of PD. (A) SNH-related diagnostic classification model. (B) CRP-related diagnostic classification model. (C) Hcy-related diagnostic classification model.

biomarkers CRP and Hcy, significantly improving the diagnostic performance of PD-CI risk stratification. This diagnostic classification model not only provides clinical targets for individualized intervention but also optimizes CI risk stratification and clinical pathways. Additionally, this study provides some research support for the mechanism gap in ultrasound technology for PD-CI diagnosis, as SNH-reflected substantia nigra iron deposition and abnormal inflammatory markers may support the hypothesis of the "iron deposition-neuroinflammation-CI" circuit.

This study indicates that patients <50 years had 83% lower odds of CI than those ≥75 years. Neurodegenerative processes in PD are thought to accelerate brain aging and alter cognitive trajectories, with older adults exhibiting more pronounced cognitive decline [25]. A cohort of patients with Parkinson's disease in Spain cohort study reported predicted age differences of 7.08 years in gray matter and 8.82 years in white matter among patients with PD-CI [26]. This study corroborates the aforementioned research, emphasizing the heterogeneous impact of aging on cognitive decline

in PD. However, a key distinction is that the cognitive protective association in early-onset PD (<50 years) was not moderated by years of education or the measured biomarkers, suggesting that age <50 years itself may confer an independent neuroprotective effect.

Each additional year of formal education was associated with a 12.2% reduction in the odds of PD-CI. These results are consistent with a prior study indicating that higher educational attainment is associated with better cognitive function and reduced dementia risk, even in the presence of neurodegenerative disease [27]. Educational attainment influences cognitive trajectories, with higher levels associated with better working memory and subcortical task performance, greater compensatory capacity of the frontostriatal circuit, enhanced dopaminergic efficiency, and greater cognitive reserve [26]. In the Proceedings of the National Academy of Sciences, Schwarzacher and colleagues showed that repetitive neural activity induced by learning expands synapses on dendritic spines, strengthening neuronal connections. This synaptic plasticity helps stabilize neuronal activity and supports cognitive function [28].

Additionally, each one-point increase in the UPDRS-III score corresponded to a 2.4% increase in the odds of PD-CI. From an effect-size perspective, the impact may be modest at low UPDRS-III scores, but cumulative effects at higher scores can meaningfully increase the odds of PD-CI (e.g., ~48% higher odds for a 20-point increase from 30 to 50). These cumulative effects have clear implications for clinical intervention. Furthermore, as the gold standard for assessing motor symptoms, an increase in UPDRS-III scores reflects worsening degeneration of the cortical-basal ganglia-thalamic circuit (CBTC) [29]. The observed association between PD-CI and UPDRS-III deepens understanding of the scale's diagnostic performance, as score changes mark motor deterioration and may also indicate cognitive decline via motor-cognitive neural circuits [30].

SNH serves as an imaging marker for SN iron deposition, with a sensitivity of 60.56% and specificity of 66.67%, consistent with a previous TCS study [15]. The high specificity of CRP and Hcy (88.10% and 83.33%, respectively) further supports the significant role of neuroinflammation in PD-CI [31–33]. Additionally, the SNH+CRP+Hcy diagnostic classification model demonstrated improved AUCs (PD-CI: 0.783; PD-MCI: 0.729; PD-dementia: 0.823), with the most significant gain observed for PD-dementia. This pattern may reflect synergistic effects of multiple pathway biomarkers amplified by widespread corticolimbic degeneration [34]. This mechanism aligns with proteomics findings of abnormal plasma H3C15 (histone-associated neuroinflammation) and PSAP (lysosomal dysfunction) in PD dementia patients, suggesting that multimodal biomarkers reflect interplay between neurodegenerative and inflammatory pathways [35].

Notably, SNH, CRP, and Hcy were independent risk factors for PD-CI, with a gradient in effect sizes: SNH-positive cases had 2.55-fold higher odds (OR = 2.550), elevated CRP conferred 2.04-fold higher odds (OR = 2.038), and elevated Hcy had the strongest association (OR = 2.830; 2.83-fold higher odds). These factors may collectively participate in an "iron deposition-neuroinflammation-CI" circuit: SNH reflects iron deposition in the SN, which activates microglia and promotes release of inflammatory mediators (e.g., IL-1β), CRP, as a systemic marker, is linked to blood-brain barrier disruption and neurodegeneration, and Hcy synergistically promotes cognitive decline via oxidative stress and tau hyperphosphorylation [36–38]. SNH serves as a structural marker, while CRP and Hcy are dynamic inflammation-associated indicators, and the three factors synergistically amplify the risk of cognitive decline in PD.

Quantitative susceptibility mapping (QSM) on MRI provides supporting evidence for links between iron deposition and CI-related circuits. Voxel-based QSM study has shown that, relative to PD with normal cognition, PD-MCI exhibits higher susceptibility in the cuneus, precuneus, caudate head, fusiform gyrus, and orbitofrontal cortex, and susceptibility in these regions is inversely associated with MoCA scores, indicating structural and functional links between iron burden and cognitive deficits [39]. A subsequent study has linked QSM-derived iron metrics to the severity and progression of cognitive impairment in PD, suggesting a pathological connection between iron dyshomeostasis and dysfunction of corticostriatal networks [40]. These observations align with the present framework: SNH primarily reflects nigral iron deposition and glial activation, providing a PD-specific anchor for peripheral inflammation-related signals, whereas QSM quantifies iron burden in key extranigral circuits (including cortical and striatal regions), complementing ultrasound by addressing limitations in spatial resolution and quantification for mechanistic interpretation.

The core clinical insight of this study is the development of a CI-oriented diagnostic framework that integrates SNH measured by transcranial sonography with the inflammatory biomarkers CRP and Hcy, providing a practical avenue for early screening and more precise intervention in PD. In PD patients at lower risk of CI, the SNH+CRP/Hcy combination achieves a sensitivity of 76.76%–80.28% in the PD-CI group. When all three markers are combined, the AUC increases to 0.783, enabling efficient preliminary screening. For high-risk PD populations (such as those with RBD or olfactory dysfunction), the SNH+CRP/Hcy combination achieves a sensitivity of 84.15% in the PD-dementia group. When all three are combined, the AUC reaches 0.823, maximizing the identification of early cognitive decline signals. In specialized clinical settings, the SNH+CRP+Hcy model demonstrates balanced performance, supporting the accurate identification of PD-dementia. Because transcranial sonography is simple, safe, and cost-effective, combining it with readily avail-

able blood markers yields a screening protocol suitable for primary care and may reduce costs compared with strategies relying on cerebrospinal fluid testing or advanced imaging. This panel is positioned as a complement to the Montreal Cognitive Assessment, allowing integration into standardized PD assessment pathways and enabling prioritization of neuropsychological testing and shorter follow-up intervals when MoCA results are normal or borderline but clinical concern persists. This approach may help address limitations of single neuropsychological assessments and enable earlier identification of cognitive impairment in PD, thereby guiding clinical decisions.

This study has limitations. First, follow-up data were not available. However, as a cross-sectional study, the research focused on evaluating the diagnostic performance of the SNH and inflammation-associated biomarker model rather than disease-progression trajectories. Multivariable logistic regression controlled for time-related variables (e.g., disease duration and age), and the model maintained significant diagnostic power across CI stages, supporting the robustness of the conclusions. Future work will employ longitudinal cohorts, combining MoCA subscale scores with dynamic biomarker changes to construct a temporal risk model for cognitive decline. Second, cognitive status was defined using MoCA cutoffs for pragmatic, reproducible multicenter evaluation of model discrimination, rather than diagnostic confirmation by comprehensive neuropsychological assessment. Because MoCA may be influenced by education, we interpret education-related findings as screening-based associations rather than a causal "protective" effect. Third, the sample size was modest, increasing the risk of overfitting. Nevertheless, credibility is supported by a parsimonious, clinically prespecified set of covariates. Effect directions and magnitudes were consistent across cognitive strata. Evidence converged across independent modalities, including SNH and inflammation-related biomarkers. AUC estimates and their confidence intervals were clearly above chance. Findings support the model's potential to guide early risk stratification and clinical decision-making, while underscoring the need for confirmation in larger prospectively validated cohorts and external validation studies. Future studies will expand sample size through multicenter collaboration to enhance generalizability.

5. Conclusion

In conclusion, a diagnostic classification model based on ultrasound-derived SNH and the inflammation-associated biomarkers CRP and Hcy was proposed, establishing a framework for stratified diagnosis of CI stage in PD. This framework may provide clinical targets for individualized intervention and help optimize PD risk stratification and clinical pathways.

Availability of Data and Materials

The data that support the findings of this study are available from the corresponding author upon reasonable request.

Author Contributions

WH and WZ conceived and designed the study, provided study materials/patients, and provided administrative support. JZ conceived and designed the study and provided study materials/patients. JZ, YL, SW and LX collected and assembled the data. JZ and CH analyzed and interpreted the data. All authors drafted the manuscript or revised it critically for important intellectual content. All authors read and approved the final version to be published. All authors participated sufficiently in the work and agreed to be accountable for all aspects of the work, ensuring that any questions related to the accuracy or integrity of any part of the work are appropriately investigated and resolved.

Ethics Approval and Consent to Participate

The study protocol was approved by the Institutional Board of Beijing Tiantan Hospital, Capital Medical University (approval No. KY2022-015-04). Informed consent was obtained from all participants. All procedures involving human participants were conducted in accordance with the ethical standards of the institutional research committee and the Declaration of Helsinki (1964) and its later amendments or comparable ethical standards.

Acknowledgment

Not applicable.

Funding

This work was supported by the National Natural Science Foundation of China (No. 82271995 and 81730050).

Conflict of Interest

The authors declare no conflict of interest.

Supplementary Material

Supplementary material associated with this article can be found, in the online version, at https://doi.org/10.31083/JIN46585.

References

[1] Zaman V, Shields DC, Shams R, Drasites KP, Matzelle D, Haque A, *et al*. Cellular and molecular pathophysiology in the progression of Parkinson's disease. Metabolic Brain Disease. 2021; 36: 815–827. https://doi.org/10.1007/s11011-021-00689-5.

[2] Aarsland D, Batzu L, Halliday GM, Geurtsen GJ, Ballard C, Ray Chaudhuri K, *et al*. Parkinson disease-associated cognitive impairment. Nature Reviews. Disease Primers. 2021; 7: 47. https://doi.org/10.1038/s41572-021-00280-3.

[3] Chandler JM, Nair R, Biglan K, Ferries EA, Munsie LM, Changamire T, *et al*. Characteristics of Parkinson's Disease in Patients with and without Cognitive Impairment. Journal of Parkinson's Disease. 2021; 11: 1381–1392. https://doi.org/10.3233/JPD-202190.

[4] Vossius C, Larsen JP, Janvin C, Aarsland D. The economic impact of cognitive impairment in Parkinson's disease. Movement Disorders: Official Journal of the Movement Disorder Society. 2011; 26: 1541–1544. https://doi.org/10.1002/mds.23661.

[5] Jellinger KA. Pathobiology of Cognitive Impairment in Parkinson Disease: Challenges and Outlooks. International Journal of Molecular Sciences. 2023; 25: 498. https://doi.org/10.3390/ijms25010498.

[6] Schumacher J, Kanel P, Dyrba M, Storch A, Bohnen NI, Teipel S, *et al*. Structural and molecular cholinergic imaging markers of cognitive decline in Parkinson's disease. Brain: a Journal of Neurology. 2023; 146: 4964–4973. https://doi.org/10.1093/brain/awad226.

[7] Delgado-Alvarado M, Ferrer-Gallardo VJ, Paz-Alonso PM, Caballero-Gaudes C, Rodríguez-Oroz MC. Interactions between functional networks in Parkinson's disease mild cognitive impairment. Scientific Reports. 2023; 13: 20162. https://doi.org/10.1038/s41598-023-46991-3.

[8] Periñán MT, Macías-García D, Jesús S, Martín-Rodríguez JF, Muñoz-Delgado L, Jimenez-Jaraba MV, *et al*. Homocysteine levels, genetic background, and cognitive impairment in Parkinson's disease. Journal of Neurology. 2023; 270: 477–485. https://doi.org/10.1007/s00415-022-11361-y.

[9] Lin WZ, Yu D, Xiong LY, Zebarth J, Wang R, Fischer CE, *et al*. Homocysteine, neurodegenerative biomarkers, and APOE ε4 in neurodegenerative diseases. Alzheimer's & Dementia: the Journal of the Alzheimer's Association. 2025; 21: e14376. https://doi.org/10.1002/alz.14376.

[10] Gu L, Luo WY, Xia N, Zhang JN, Fan JK, Yang HM, *et al*. Up-regulated mGluR5 induces ER stress and DNA damage by regulating the NMDA receptor subunit NR2B. Journal of Biochemistry. 2022; 171: 349–359. https://doi.org/10.1093/jb/mvab140.

[11] Rosell-Díaz M, Santos-González E, Motger-Albertí A, Gallardo-Nuell L, Arnoriaga-Rodríguez M, Coll-Martínez C, *et al*. Lower serum ferritin levels are associated with worse cognitive performance in aging. The Journal of Nutrition, Health & Aging. 2024; 28: 100190. https://doi.org/10.1016/j.jnha.2024.100190.

[12] Li Y, Ruan X, Sun M, Yuan M, Song J, Zhou Z, *et al*. Iron deposition participates in LPS-induced cognitive impairment by promoting neuroinflammation and ferroptosis in mice. Experimental Neurology. 2024; 379: 114862. https://doi.org/10.1016/j.expneurol.2024.114862.

[13] Hemmati-Dinarvand M, Taher-Aghdam AA, Mota A, Zununi Vahed S, Samadi N. Dysregulation of serum NADPH oxidase1 and ferritin levels provides insights into diagnosis of Parkinson's disease. Clinical Biochemistry. 2017; 50: 1087–1092. https://doi.org/10.1016/j.clinbiochem.2017.09.014.

[14] Shen J, Amari N, Zack R, Skrinak RT, Unger TL, Posavi M, *et al*. Plasma MIA, CRP, and Albumin Predict Cognitive Decline in Parkinson's Disease. Annals of Neurology. 2022; 92: 255–269. https://doi.org/10.1002/ana.26410.

[15] Hou C, Yang F, Li S, Ma HY, Li FX, Zhang W, *et al*. A nomogram based on neuron-specific enolase and substantia nigra hyperechogenicity for identifying cognitive impairment in Parkinson's disease. Quantitative Imaging in Medicine and Surgery. 2024; 14: 3581–3592. https://doi.org/10.21037/qims-23-1778.

[16] Papuć E, Rejdak K. Increased Cerebrospinal Fluid S100B and NSE Reflect Neuronal and Glial Damage in Parkinson's Disease. Frontiers in Aging Neuroscience. 2020; 12: 156. https://doi.org/10.3389/fnagi.2020.00156.

[17] Hou C, Zhang W, Li HB, Li S, Nie F, Wang XM, *et al*. Spatial variations and precise location of substantia nigra hyperechogenicity in Parkinson's disease using TCS-MR fusion imaging. NPJ Parkinson's Disease. 2025; 11: 78. https://doi.org/10.1038/s41531-025-00910-7.

[18] Yin Y, Tian N, Deng Z, Wang J, Kuang L, Tang Y, *et al*. Targeted Microglial Membrane-Coated MicroRNA Nanosponge Mediates Inhibition of Glioblastoma. ACS Nano. 2024; 18: 29089–29105. https://doi.org/10.1021/acsnano.4c10509.

[19] Kals M, Reigo A, Teder-Laving M, Vaht M, Estonian Biobank research team, Nikopensius T, *et al*. Polygenic Risk Score Combined with Transcranial Sonography Refines Parkinson's Disease Risk Prediction. Movement Disorders Clinical Practice. 2025; 12: 928–937. https://doi.org/10.1002/mdc3.70011.

[20] Postuma RB, Berg D, Stern M, Poewe W, Olanow CW, Oertel W, *et al*. MDS clinical diagnostic criteria for Parkinson's disease. Movement Disorders: Official Journal of the Movement Disorder Society. 2015; 30: 1591–1601. https://doi.org/10.1002/mds.26424.

[21] Skorvanek M, Goldman JG, Jahanshahi M, Marras C, Rektorova I, Schmand B, *et al*. Global scales for cognitive screening in Parkinson's disease: Critique and recommendations. Movement Disorders: Official Journal of the Movement Disorder Society. 2018; 33: 208–218. https://doi.org/10.1002/mds.27233.

[22] Lilja G, Ullén S, Dankiewicz J, Friberg H, Levin H, Nordström EB, *et al*. Effects of Hypothermia vs Normothermia on Societal Participation and Cognitive Function at 6 Months in Survivors After Out-of-Hospital Cardiac Arrest: A Predefined Analysis of the TTM2 Randomized Clinical Trial. JAMA Neurology. 2023; 80: 1070–1079. https://doi.org/10.1001/jamaneurol.2023.2536.

[23] Avila Pérez S, Koppelmans V, Duff KM, Ruitenberg MF. One-year practice effects predict long-term cognitive outcomes in Parkinson's disease. Journal of Parkinson's Disease. 2025; 15: 858–867. https://doi.org/10.1177/1877718X251339585.

[24] Bartova P, Skoloudik D, Bar M, Ressner P, Hlustik P, Herzig R, *et al*. Transcranial sonography in movement disorders. Biomedical Papers of the Medical Faculty of the University Palacky, Olomouc, Czechoslovakia. 2008; 152: 251–258. https://doi.org/10.5507/bp.2008.039.

[25] Gallagher J, Gochanour C, Caspell-Garcia C, Dobkin RD, Aarsland D, Alcalay RN, *et al*. Long-Term Dementia Risk in Parkinson Disease. Neurology. 2024; 103: e209699. https://doi.org/10.1212/WNL.0000000000209699.

[26] Chen CL, Cheng SY, Montaser-Kouhsari L, Wu WC, Hsu YC, Tai CH, *et al*. Advanced brain aging in Parkinson's disease with cognitive impairment. NPJ Parkinson's Disease. 2024; 10: 62. https://doi.org/10.1038/s41531-024-00673-7.

[27] Kotagal V, Bohnen NI, Müller MLTM, Koeppe RA, Frey KA, Langa KM, *et al*. Educational attainment and motor burden in Parkinson's disease. Movement Disorders: Official Journal of the Movement Disorder Society. 2015; 30: 1143–1147. https://doi.org/10.1002/mds.26272.

[28] Casaletto KB, Rentería MA, Pa J, Tom SE, Harrati A, Armstrong NM, *et al*. Late-Life Physical and Cognitive Activities Independently Contribute to Brain and Cognitive Resilience. Journal of Alzheimer's Disease: JAD. 2020; 74: 363–376. https://doi.org/10.3233/JAD-191114.

[29] Wang Y, Jiang Z, Chu C, Zhang Z, Wang J, Li D, *et al*. Push-pull effects of basal ganglia network in Parkinson's disease inferred by functional MRI. NPJ Parkinson's Disease. 2024; 10: 224. https://doi.org/10.1038/s41531-024-00835-7.

[30] Ferrazzoli D, Ortelli P, Volpe D, Cucca A, Versace V, Nardone R, *et al*. The Ties That Bind: Aberrant Plasticity and Networks Dysfunction in Movement Disorders-Implications for Rehabilitation. Brain Connectivity. 2021; 11: 278–296. https://doi.org/10.1089/brain.2020.0971.

[31] Hayek D, Ziegler G, Kleineidam L, Brosseron F, Nemali A, Vockert N, *et al*. Different inflammatory signatures based on CSF biomarkers relate to preserved or diminished brain structure and cognition. Molecular Psychiatry. 2024; 29: 992–1004. https://doi.org/10.1038/s41380-023-02387-3.

[32] Luo J, le Cessie S, Blauw GJ, Franceschi C, Noordam R, van Heemst D. Systemic inflammatory markers in relation to cognitive function and measures of brain atrophy: a Mendelian randomization study. GeroScience. 2022; 44: 2259–2270. https://doi.org/10.1007/s11357-022-00602-7.

[33] Allen WE, Blosser TR, Sullivan ZA, Dulac C, Zhuang X. Molecular and spatial signatures of mouse brain aging at single-cell resolution. Cell. 2023; 186: 194–208.e18. https://doi.org/10.1016/j.cell.2022.12.010.

[34] McGregor MM, Nelson AB. Circuit Mechanisms of Parkinson's Disease. Neuron. 2019; 101: 1042–1056. https://doi.org/10.1016/j.neuron.2019.03.004.

[35] Yang B, Zhu Y, Li K, Wang F, Liu B, Zhou Q, *et al*. Machine learning model base on metabolomics and proteomics to predict cognitive impairment in Parkinson's disease. NPJ Parkinson's Disease. 2024; 10: 187. https://doi.org/10.1038/s41531-024-00795-y.

[36] Yang X, Wang M, Liu W, Hou M, Zhao J, Huang X, *et al*. Quantitative susceptibility mapping in rats with minimal hepatic encephalopathy: Does iron overload aggravate cognitive impairment by promoting neuroinflammation? NeuroImage. 2023; 283: 120418. https://doi.org/10.1016/j.neuroimage.2023.120418.

[37] Wilcockson TDW, Roy S. Could Alcohol-Related Cognitive Decline Be the Result of Iron-Induced Neuroinflammation? Brain Sciences. 2024; 14: 520. https://doi.org/10.3390/brainsci14060520.

[38] Zhang C, Hu Y, Cao X, Deng Y, Wang Y, Guan M, *et al*. Lower water-soluble vitamins and higher homocysteine are associated with neurodegenerative diseases. Scientific Reports. 2025; 15: 18866. https://doi.org/10.1038/s41598-025-03859-y.

[39] Uchida Y, Kan H, Sakurai K, Arai N, Kato D, Kawashima S, *et al*. Voxel-based quantitative susceptibility mapping in Parkinson's disease with mild cognitive impairment. Movement Disorders: Official Journal of the Movement Disorder Society. 2019; 34: 1164–1173. https://doi.org/10.1002/mds.27717.

[40] Thomas GEC, Leyland LA, Schrag AE, Lees AJ, Acosta-Cabronero J, Weil RS. Brain iron deposition is linked with cognitive severity in Parkinson's disease. Journal of Neurology, Neurosurgery, and Psychiatry. 2020; 91: 418–425. https://doi.org/10.1136/jnnp-2019-322042.